VOL. 13, NO. 7, APRIL 2018 ISSN 1819-6608
ARPN Journal of Engineering and Applied Sciences

www.arpnjournals.com

EXPERIMENTAL STUDY ON FLOW AROUND AIRFOIL BY USING DIELECTRIC BARRIER DISCHARGE (DBD) PLASMA ACTUATOR

Farah Ayiesya Zainuddin[1, 2], Nazri Md Daud[1, 2], Shafizal Mat[1, 2] and Zolkafle Buntat[3]
[1]Centre for Advanced Research on Energy, Universiti Teknikal Malaysia Melaka, Hang Tuah Jaya, Durian Tunggal, Melaka, Malaysia
[2]Faculty of Mechanical Engineering, Universiti Teknikal Malaysia Melaka, Hang Tuah Jaya, Durian Tunggal, Melaka, Malaysia
[3]Institut of High Voltage and High Current (IVAT), Faculty of Electrical Engineering, Universiti Teknologi Malaysia, UTM Johor Bahru, Malaysia
E-Mail: nazridaud@utem.edu.my

ABSTRACT

This experimental study was focused on the usage of DBD plasma actuator for enhancement aerodynamic performance of airfoil model NACA 0015. The DBD plasma actuator was able to suppress flow separation near the leading edge by disturbing airflow near that region. It can be seen that continuous small scale vortex is produced near the leading edge and it flows near the airfoil surface. Experimental works were performed at Reynold number approximately 63000 to 252000 with external airflow 5 m/s, 15 m/s, and 20 m/s. A thin plasma actuator was installed on NACA 0015 with 190 mm chord length and 260 mm span length at $x/c = 0.025$, where x is the vertical distance measured from leading edge and c was the chord length. Lift force measurement, measurement of pressure distribution on upper surface of airfoil and flow visualization were conducted to investigate the effectiveness of DBD plasma actuator. The experiment was tested during plasma ON (actuation) and plasma OFF (baseline case). The result shows that actuation case may increase lift coefficient compare to baseline case.

Keywords: dielectric barrier discharge, plasma actuator, airfoil, separation control.

INTRODUCTION

Active flow control by DBD plasma actuator is currently studied in order to control external airflow on aerodynamic geometries. Plasma is created when electrodes are energized at high voltage and frequency, causing airflow over the embedded electrode ionize and then induces a jet flow (Jukes and Choi, 2006).

DBD plasma actuator can be used in various application such as control the airflow separation on airfoil under laminar flow (Sosa and Artana, 2006; Md Daud *et al.*, 2016), optimize the actuator position (Jolibois et al., 2008), reattachment of airflow (Jukes and Choi, 2006), separation control using unsteady actuation (Amitay and Glezer,2002; Rethmel *et al.*, 2011; Md Daud *et al.*, 2016) and increase the lift and drag performance of airfoils (Benard et al., 2009). The special features of this actuation were having no moving parts, light weight, easily to fabricate and their ability to respond instantly. Therefore, its become a famous flow control device for application on aircraft. Next, DBD plasma actuator could reduce fuel consumption and contribute to green environment by achieving high aerodynamic performance.

DBD plasma actuator consists of dielectric barrier between two electrodes, an exposed and insulated electrode, a high voltage and high frequency AC power supply. The configuration of actuator is shown in Figure-1. The two electrodes are slightly overlapped. Plasma is created when enough voltage is supplied between the electrodes. Momentum is transferred from the plasma discharge to surrounding through a collision of ions that produce induced air and body force. Interaction of electrochemical occurs between plasma and air causes plasma kinetic phenomenon due to existing low density of electrons, positive ions, negative ions and neutral particles (Wang *et al.*, 2007). The term "plasma" is used because ionization occurs and it refers to plasma. Blue color appears when air is ionized due to recombination of air and de-excite to ionized components (Davidson and O'Neil, 1964). The DBD plasma actuator can be turned ON and OFF as required.

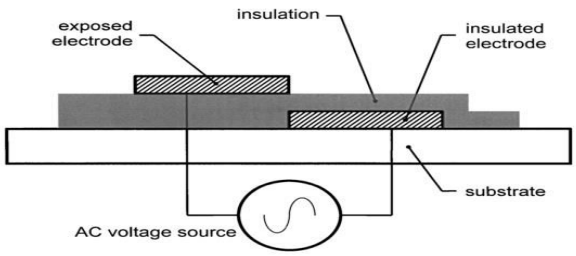

Figure-1. Asymmetric actuator arrangement of electrodes, one of which is insulated, on an aerodynamic surface (Enloe *et al.*, 2004).

By placing the DBD plasma actuator near the leading or trailing edge as a plasma flap (He *et al.*, 2009) this will improve the aerodynamic performance of airfoil that function as separation control device (Post and Corke, 2006;Sosa *et al.*, 2007). This method can increase the lift coefficient on airfoil. The concept of "virtual section shape" has been proposed (He et al., 2009) and at the same time, the actuator can be used as vortex generator to control flow over an airfoil (Okita *et al.*, 2008).

Forte *et al.*, (2007) conducted measurement by using pitot tube and found an ionic velocities up to 7 m/s at 0.5mm from wall for single actuator while 8 m/s for multiple actuators. Besides, Hale *et al.* (2010) came out with new configuration for plasma actuator where they claimed the biggest problem using this actuator is relatively low induced velocity of the jet. When the jet

velocity increased, more momentum can be imparted to the flow. Therefore, by increasing the jet velocity this device is suitable to be used for wider range of Reynolds numbers. They studied the potential of multiple encapsulated electrodes (MEE) to increase the induced velocity. From the result, they able to use MEE actuators to produce an induced velocity that was 36.5% higher than baseline case. However, a higher ionic velocity is not strictly related to improve flow control performance (Benard et al., 2009). They found that unsteady actuation increase aerodynamic performance of airfoil compared to steady actuation. There is stronger suspicion that the vortex interaction has a larger influence on improved results than ionic velocity.

Jukes and Choi (2012) showed a DBD vortex generator developed streamwise vortices in their experiments. They successfully used their method to reduce the separation region. Therefore, the vortex interaction due to actuation effect or actuator position was important for improving the flow control performance.

For this case, the DBD plasma actuator was placed near the leading edge of the NACA 0015 airfoil model. Therefore, the purpose of this study was to improve a lift coefficient by comparing the result of lift, pressure distribution, and flow visualization for actuation and baseline case.

METHODOLOGY

This section describes the methodology of project to prove the effectiveness of DBD plasma actuator on leading edge of airfoil. The comparison is made when plasma is ON and OFF.

Experiment setup

The experiment was conducted in two types of low speed, semi-closed wind tunnel with a square cross section having dimension of 457 mm × 457 mm for lift and pressure distribution experimental. From the Figure 2, as to minimize the end of effects, end exhibits well-behaved the acrylic plates with 2 mm thickness are mounted on the sides of the airfoil to allow visual access for and measurement. While, the airflow visualization on NACA 0015 used the semi–closed wind tunnel with a square test section 300 mm × 300 mm. A NACA 0015 was used with chord length 190 mm and span length 260 mm as in Figure-2. The experiment was tested at approximately $Re \approx$ 189000 to 252000 with velocity 15 m/s and 20 m/s for lift and pressure distribution experiment. The wind tunnel speed was monitored using a pitot-static tube placed upstream of models mounted within test section.

While, for the flow visualization experiment, 5 m/s external airflow was used. The experiment was tested at approximately $Re \approx 63000$. The Reynolds number was selected to allow us understand the effect of plasma actuator on the flow around airfoil and clarify the separation control mechanism in flight application with low Reynolds number (Sosa and Artana, 2006; Yang *et al.*, 2007; Greenblatt *et al.*, 2008). The DBD plasma actuator was installed near the leading edge at $x/c = 0.025$ of the chord length. The end of the plates was made by thick clear acrylic material to enable visualization of the flow.

DBD plasma actuator consists of two copper tape electrodes with 10mm wide and 50µm thick as shown in the Figure-2. The exposed and embedded electrodes were arranged parallel with 1mm overlap. For the dielectric barrier, kapton film with 100µm was used. A high voltage AC current was supplied to the exposed electrode and embedded electrode was grounded. The high output voltage device was used in this project. With only 240 V, 50/60 Hz input, the output of the circuit can reach up until 6 kV with frequency 20 kHz.

Flow visualization was conducted by using high speed camera (Phantom v710) and continuous light from led lamp with it driver (BZ-8/12X1W). The led lamp intersected at airfoil of mid-span, and the axis of speed camera was perpendicular to led lamp. The camera frame was rate over 7500 frames-per-second (fps) with full megapixel resolution.

From the Figure-3, the space inside of wind tunnel was filled with a smoke filament. The tunnel blockage effect on the aerodynamic coefficients considered minimal and no correction in measurements were necessary (Erfani and Keshmiri, 1998).

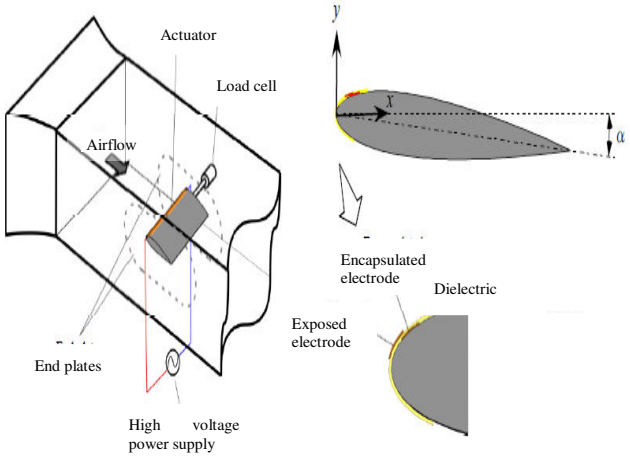

Figure-2. Experiment setup using airfoil model NACA 0015 in a low- speed, semi closed wind tunnel with $Re \approx$ 189000 to 252000 with velocity 15 m/s and 20 m/s.

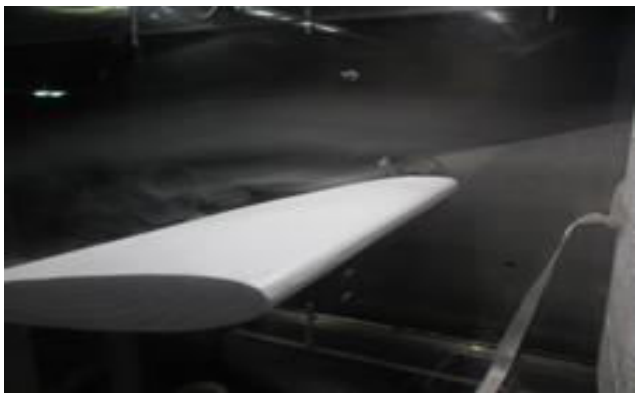

Figure-3. Test section wind tunnel filled a smoke filament.

Coefficient of lift

This section discusses the effect of DBD plasma actuator on NACA 0015 by comparing the lift coefficient when plasma ON or OFF. By using only 240 V, 50/60 Hz input high voltage alternating current (a. c); the output can reach up until 6kV with frequency 20kHz. The instantaneous lift force obtained from dynamic force balance measurement.

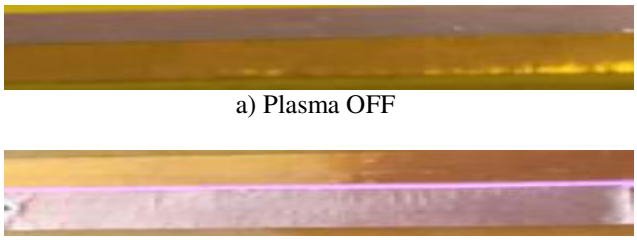

a) Plasma OFF

b) Plasma ON

Figure-4. The actuation (plasma ON) and baseline case (plasma OFF).

Coefficient of lift (C_L), were produced by calculation from result of lift force. These aerodynamic coefficients are commonly defined as:

$$C_L = L / 0.5\rho U_o^2 S \quad (1)$$

$$S = \text{chord} \times \text{span} \quad (2)$$

where L refers to the lift force and was determined from time-averaged force measurement ; ρ is air density, U_o is a free stream velocity, S is a lifting area chord times by a span length (Leroy *et al.*, 2011a). The data was used to compare the aerodynamic performance of the airfoil in the presence or in absence of plasma discharge.

Pressure measurement

The pressure along the airfoil surface (P_i) was measured by 7 pressure ports that were drilled at the half of the span location of the airfoil. The tapped holes diameter was 1mm and the tubes were inserted in the holes passed through the hollow of airfoil and brought out through one end support of the model. The static pressure of the freestream (P_O) was taken using a micromanometer (DP-CALC^{TM} 5825). The holes are located at upper surface only because this measurement of pressure only made for upper part.

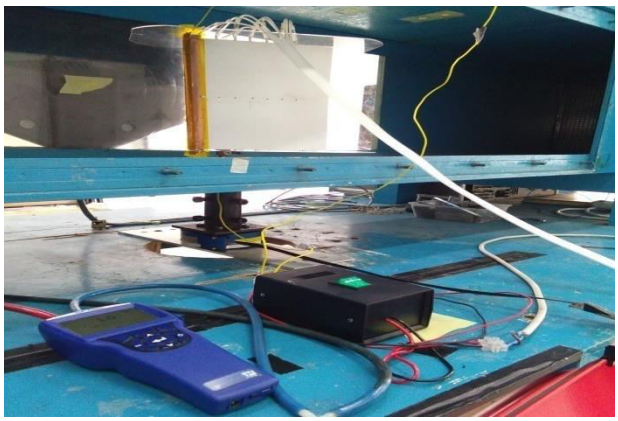

Figure-5. NACA 0015 model with7 pressure ports.

In this study, the pressure coefficient C_P is defined as:

$$C_P = (P_i - P_O)/0.5\rho U^2_O \quad (3)$$

where P_i is the surface pressure at station i, ρ the gas density, and U_O the free stream velocity (Sosa and Artana, 2006). In regions where the flow was separated, the surface pressure at the different ports was unsteady and the value of the pressure considered there was a time-averaged value obtained by the direct measurement.

Flow visualization

The flow visualization at low speed velocities was utilized paraffin oil to generate a smoke filament. This allows creation of a smoke in space of test section and a led lamp assists the visualization of the smoke filament. This led lamp mounted on the upper surface of test section. The flow visualization was recorded with high speed camera (Phantom v710).

RESULTS AND DISCUSSIONS

Effect of DBD plasma actuator on lift coefficient

Figures 6 and 7 show, the C_L for baseline case (plasma OFF) and with actuation (plasma ON). The graph was plotted by C_L against the angle of attack, α. From the both graph the C_L increases with angle of attack up to 16° and then reduce gradually loss in lift is observed. The C_L improved for the entire angle of attack tested when plasma was ON. While, the effect of plasma to delay a stall longer than baseline case is clearly seen that C_L falls after reaching 16°. From observation, the airfoil in baseline case and actuation case were stalled at α = 16°. Even though, the stall not able to delay longer, the presented of plasma gave the effect on performance towards coefficients of lift. From the literatures review, there is a reason the delay cannot occur such that it is due to the limitation of power supply.

The graph in Figure-6 shows the maximum C_L (stall control condition) when plasma ON was approximately at 2. While, when plasma OFF the maximum C_L (stall control condition) was approximately at 1.9. From the graph, it can be seen that coefficient from entire α is increases when plasma is ON. The graph in Figure-7 shows the maximum C_L (stall control condition) when plasma is ON was approximately at 1.04. While, when plasma OFF the maximum C_L (stall control condition) was approximately at 1.0. Therefore, when velocity was at 15 m/s C_L was higher compared C_L at 20 m/s airflow. Therefore, it can be concluded that when velocity is lower the lift coefficient is much higher.

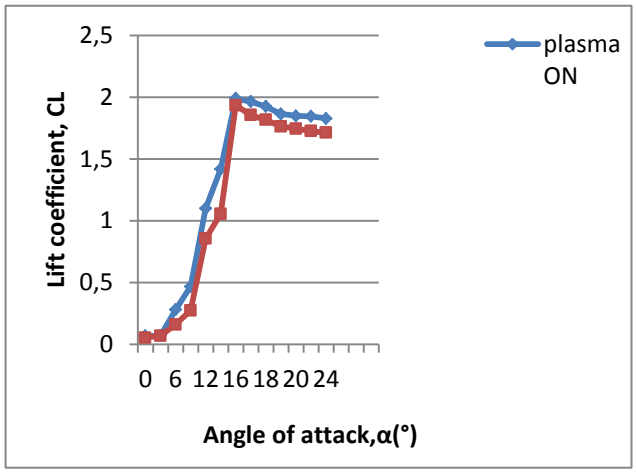

Figure-6. Graph of C_L (at velocity 15 m/s).

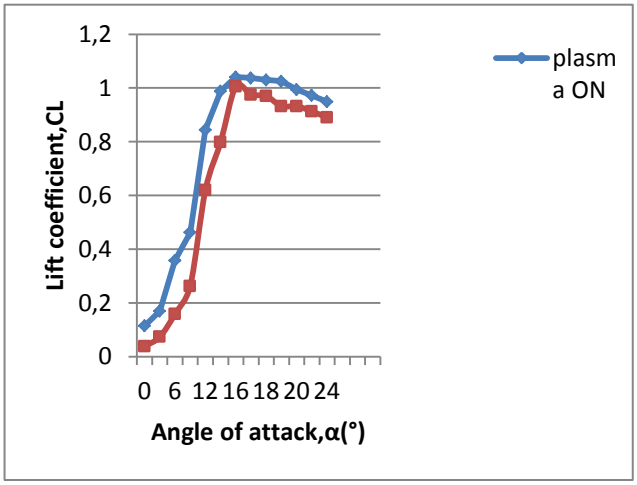

Figure-7. Graph of C_L (at velocity 20 m/s).

Effect of DBD plasma actuator on pressure distribution

The results of the mean pressure distribution on the airfoil surface are presented in this section. For a better interpretation of the test, dimensionless pressure distribution is shown in the Figures 8, 9 and 10 with the velocity 15 m/s. From the graphs, C_P was plotted against *x/c*. Graph in Figures 8 and 9 show the C_P distribution around NACA 0015 has similar trend of graph for both plasma ON and OFF. At value 15°, 16°, 17° and 18° of α the region are quite similar because of the value of C_p are in same value area. This makes them overlapped each other's. The peak of negative pressure becomes small and leading edge pressure decrease suddenly. This trend represent that the stall can be occurred at α= 16° on Re ≈ 189000.

In the Figure-10, comparison between plasma ON and OFF were made at angle 16° (stall control condition). Unfortunately, the graph shows there is no separated region value was detected. This because of differences result value between C_P for plasma ON and OFF is too small. Eventhough, the differences are smaller, but when plasma ON the pressure is lower than plasma OFF. From the literature reviews when pressure reduces, the lift will increase (Leroy *et al.*, 2011b; Grech et al., 2013; Touchard, 2008). Example, at *x/c* = 0.23, *α*= 16°, the Cp value of plasma ON was -1.70848 and when the plasma OFF the value -1.67525.

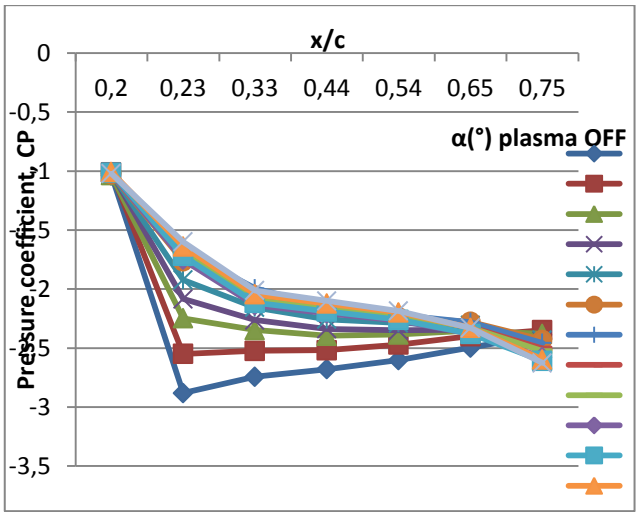

Figure-8. Graph of C_P plasma OFF (at velocity 15 m/s).

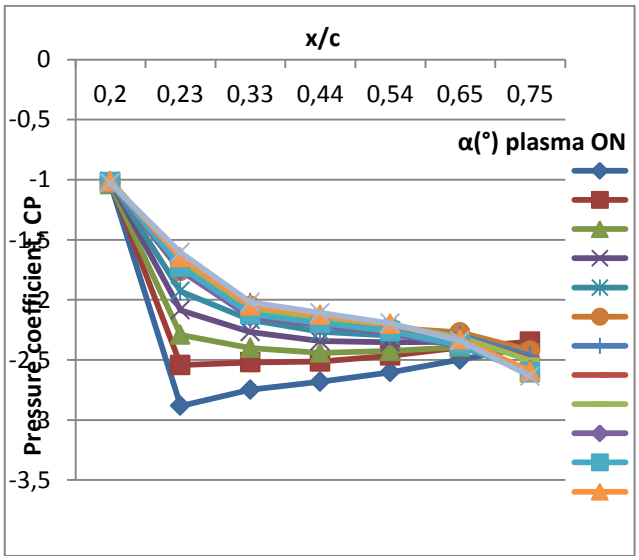

Figure-9. Graph of C_P plasma ON (at velocity 15 m/s).

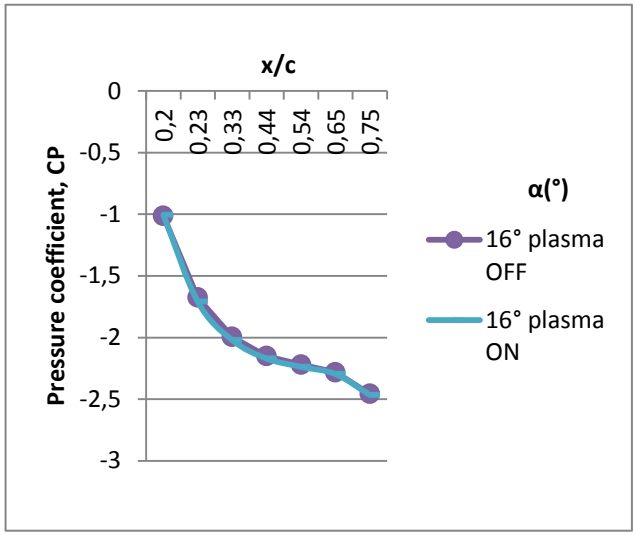

Figure-10. Graph of C_P when plasma OFF and ON (at velocity airflow 15 m/s and α= 16°).

Figures 11 and 12 show the variation of C_P at α = 16° when velocity is 20 m/s. The C_P was similar trend although with actuation or without actuation. The comparison is hardly to make because of the differences value of C_P are quite similar. But, the slope of negative pressure peak was decreased. Therefore, this can represent as the region stall occurred.

The graph in the Figure-13 does not show any difference C_P value. It is very difficult to observe the pressure distribution on the upper surface of NACA 0015. Although the plasma result of the experiment did show the conclusive decision, but it still have a small differences value of C_P between plasma ON and OFF. Example, at *x/c* = 0.23, α = 16°, the C_p value of plasma ON was -1.59801 and when the plasma OFF the value -1.59884. It shows that even though with actuation the value of C_p baseline case was lower than with actuation. One of the reason is due to the affect from velocity airflow.

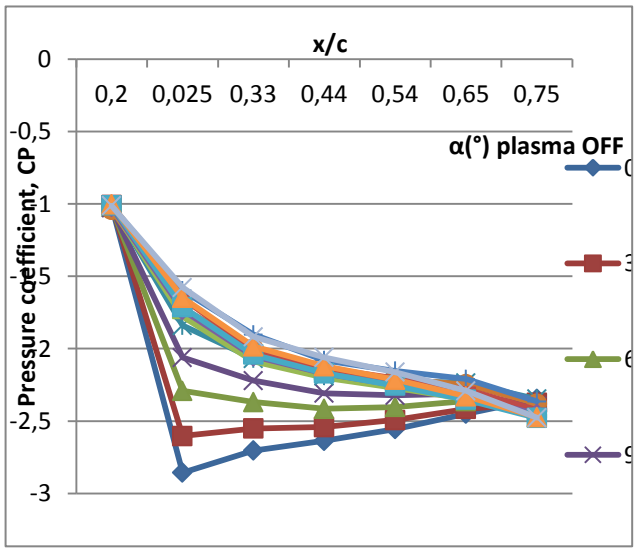

Figure-11. Graph of C_P plasma OFF (at velocity 20 m/s).

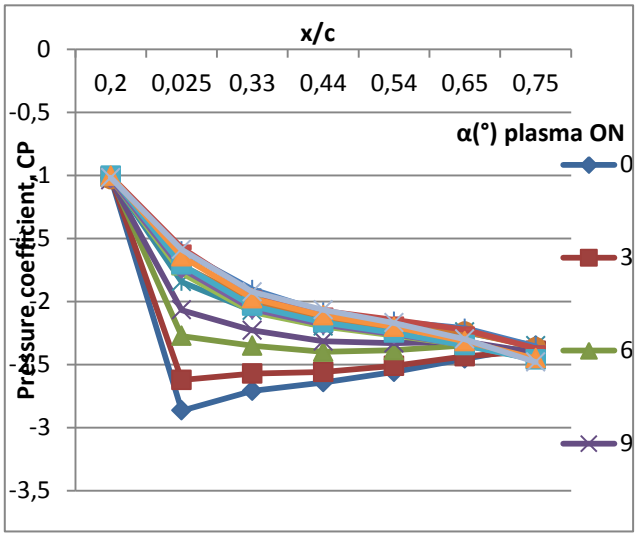

Figure-12. Graph of C_P plasma ON (at velocity 20 m/s).

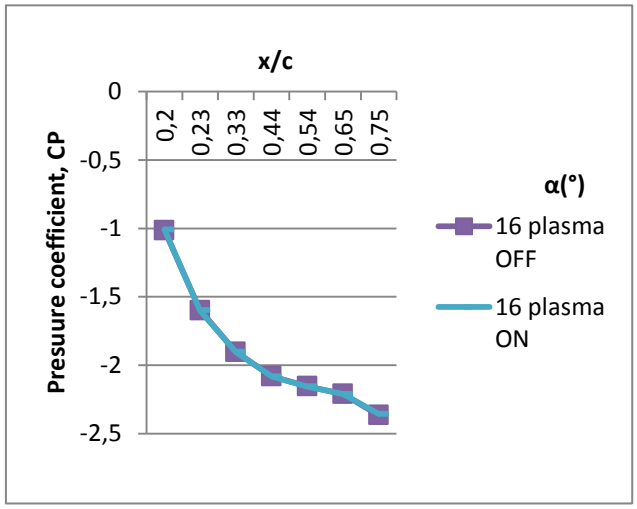

Figure-13. Graph of C_P when plasma OFF and ON (at velocity airflow 20 m/s and α= 16°).

Effect of DBD plasma actuator on flow visualization

The airflow separation control of an airfoil when DBD plasma actuator is mounted on the leading edge was examined. The actuator is applied to NACA 0015 airfoil and then flow-fields around the airfoil are visualized by using smoke generator method. From the result C_L and C_P above, the stall occurred at 16°.

The visualization of airflow with turn off the plasma were made in order to observe the effect of DBD plasma actuator on NACA 0015 as shown in the Figure-14. The external airflow used was 5 m/s with Re ≈ 63000. Averaging process gave the images of consecutives 1000 frames. From the 1000 frames, it was divided into 3 period of times to obtain the real clearly averaging frames. T is period of ON cycle. For baseline case, T is referred to be the same period as actuation case where the flow separation occurred in this case. A continuous vortex is seen to be produced near airfoil surface during T/3. Then, the vortex dispersed to downstream during 2T/3 and 3T/3. Therefore, it confirms that stall was occurred.

(a) T/3

(b) 2T/3

(c) 3T/3

Figure-14. Airflow over an airfoil when plasma OFF.

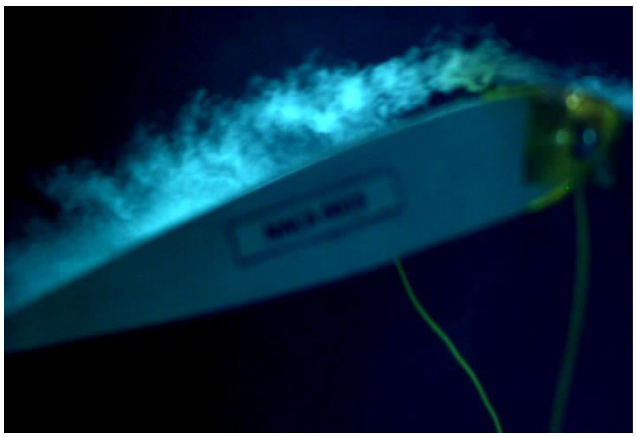

(a) T/3

(b) 2T/3

(c) 3T/3

Figure-15. Airflow over an airfoil when plasma ON.

From the Figure-15, the flow visualization with actuation was observed. Similar like the visualization flow for baseline case, the result came from averaging 1000 frames. Actuation process was able to maintain developed vortex over entire airfoil surface during T/3 and 2T/3. For 3T/3, vortex can be observed even though it is not for the entire surface. The comparison can be made between Figure 14 and 15, where the reattachment of airflow for plasma ON case is much better compared to plasma OFF.

From the Figure-15, it can be seen that actuation process produced better flow attachment compared to baseline case. The flow reattachment decreases the pressure above airfoil. As a result, it will improve the C_L. For actuation process, it can be noticed that vortex is produced from leading edge, with the airflow attach to the entire wing surface for almost T period. For baseline case, a smaller-scale vortical only developed during 1/3T and dispersed to downstream during 3T/3. From the Figures 14

and 15 it show that the flow separation result can be supported by C_L results in Figures 6 and 7. For actuation case, the separation occurs in some period of time to indicate that the stall occurred in that situation.

CONCLUSIONS

Based on this study, experimental was performed to investigate the impact of DBD plasma actuator on leading edge of NACA 0015. The results can be summarized as follows. Firstly, although the stall was not able to delay longer but the C_L for actuation case still increased compared to the baseline case. Lift coefficient is reduced slightly after reaching a maximum point.

For the pressure distribution, it is hard to see the differences of the C_P from the graph between with and without plasma. Even though the velocity was increases from 15 m/s to 20 m/s the pattern of the graph is still in same trend and the range value of result for all entire angle are not difference too much.

Lastly, the DBD plasma actuator is able to control flow separation on NACA 0015. The effectiveness of this actuator can be seen when the smoke filament can cover almost the entire of airfoil surface with presence of plasma. From the results of the experiment, it gives us conclusive decision that, with the presence of plasma by using DBD actuator the efficiency of the aerodynamic geometries can be increased.

ACKNOWLEDGEMENT

Authors would like to thank Ministry of Higher Education Malaysia and Universiti Teknikal Malaysia Melaka (UTeM) for their technical advice and suggestion. Also, special thanks to Research Acculturation Grant Scheme (RAGS/1/2015/TK0/FKM/03/B00102) for financial support.

REFERENCES

Amitay M. and Glezer A. 2002. Role of actuation frequency in controlled flow reattachment over a stalled airfoil. AIAA journal. 40(2): 209-209.

Bénard N., Jolibois J. and Moreau E. 2009. Lift and drag performances of an axisymmetric airfoil controlled by plasma actuator. Journal of Electrostatics. 67(2): 133-139.

Davidson G., and O'neil R. 1964. Optical radiation from nitrogen and air at high pressure excited by energetic electrons. The Journal of Chemical Physics. 41(12): 3946-3955.

Enloe C. L., McLaughlin T. E., VanDyken R. D., Kachner, K. D., Jumper E. J. and Corke T. C. 2004. Mechanisms and responses of a single dielectric barrier plasma actuator: plasma morphology. AIAA journal. 42(3): 589-594.

Erfani R., Keshmiri A., Erfani T. and Kontis K. 2013. Multiple Encapsulated Electrode Plasma Actuator Effect on Aerofoil-Wake Interaction. In 44th AIAA Plasmadynamics and Lasers Conference. p. 2884.

Forte M., Jolibois J., Pons J., Moreau E., Touchard G. and Cazalens M. 2007. Optimization of a dielectric barrier discharge actuator by stationary and non-stationary measurements of the induced flow velocity: application to airflow control. Experiments in Fluids. 43(6): 917-928.

Grech N., Leyland P., Peschke P. and Ott P. 2015. Investigation of flow separation control by nanosecond pulsed dielectric barrier discharge actuators. In Progress in Flight Physics–Volume 7 (Vol. 7, pp. 191-210). EDP Sciences.

Greenblatt D., Goksel B., Rechenberg I., Schule C. Y., Romann D. and Paschereit C. O. 2008. Dielectric barrier discharge flow control at very low flight Reynolds numbers. AIAA journal. 46(6): 1528.

Hale C., Erfani R. and Kontis K. 2010. Plasma actuators with multiple encapsulated electrodes to influence the induced velocity. In 48th AIAA Aerospace Sciences Meeting Including the New Horizons Forum and Aerospace Exposition, Paper Number AIAA-2010-1223.

He C., Corke T. C. and Patel M. P. 2009. Plasma flaps and slats: an application of weakly ionized plasma actuators. Journal of Aircraft. 46(3): 864.

Jolibois J., Forte M. and Moreau É. 2008. Application of an AC barrier discharge actuator to control airflow separation above a NACA 0015 airfoil: Optimization of the actuation location along the chord. Journal of Electrostatics. 66(9): 496-503.

Jukes T. N., Choi K. S., Johnson G. A. and Scott S. J. 2006. Characterization of surface plasma-induced wall flows through velocity and temperature measurements. AIAA journal. 44(4): 764-771.

Jukes T. N. and Choi K. S. 2012. Dielectric-barrier-discharge vortex generators: characterisation and optimisation for flow separation control. Experiments in fluids. 52(2): 329-345.

Leroy-Chesneau A., Audier P., Hong D., Rabat H. and Weber R. 2011, July. Effects of a surface plasma actuation on leading edge flow separation occurring on an aerodynamic airfoil involving a laminar separation bubble. In The 20th International Symposium on Plasma Chemist (pp. Paper-N).

Daud N. M., Kozato Y., Kikuchi S. and Imao S. 2016. Control of leading edge separation on airfoil using DBD plasma actuator with signal amplitude modulation. Journal of Visualization. 19(1): 37-47.

Okita Y., Jukes T. N., Choi K. S. and Nakamura K. 2008. Flow reattachment over an airfoil using surface plasma actuator. AIAA paper, 4203, 2008.

Post M. L. and Corke T. C. 2006. Separation control using plasma actuators: dynamic stall vortex control on oscillating airfoil. AIAA journal. 44(12): 3125-3135.

Rethmel C., Little J., Takashima K., Sinha A., Adamovich, I. and Samimy M. 2011. Flow separation control over an airfoil with nanosecond pulse driven DBD plasma actuators. AIAA paper, 487, 2011.

Sosa R., Artana G., Moreau E. and Touchard G. 2007. Stall control at high angle of attack with plasma sheet actuators. Experiments in fluids. 42(1): 143-167.

Sosa R. and Artana G. 2006. Steady control of laminar separation over airfoils with plasma sheet actuators. Journal of Electrostatics. 64(7): 604-610.

Touchard G. 2008. Plasma actuators for aeronautics applications-State of art review. IJ PEST. 2(1): 1-25.

Wang Y. H., Zhang Y. T., Wang D. Z. and Kong M. G. 2007. Period multiplication and chaotic phenomena in atmospheric dielectric-barrier glow discharges. Applied physics letters. 90(7): 071501.

Yang Z., Haan L. F., Hui H. and Ma H. 2007, January. An experimental investigation on the flow separation on a low-Reynolds number airfoil. In: 45th AIAA aerospace sciences meeting and exhibit. p. 275.